

Unclassified

SECURITY CLASSIFICATION OF THIS PAGE

REPORT DOCUMENTATION PAGE

1a REPORT SECURITY CLASSIFICATION Unclassified			1b RESTRICTIVE MARKINGS	
1c SECURITY CLASSIFICATION AUTHORITY LE			3 DISTRIBUTION / AVAILABILITY OF REPORT Approved for Public Release Distribution Unlimited	
AD-A203 765			5 MONITORING ORGANIZATION REPORT NUMBER(S)	
6a NAME OF PERFORMING ORGANIZATION Texas A&M University			7a NAME OF MONITORING ORGANIZATION Office of Naval Research	
6c ADDRESS (City, State, and ZIP Code) Department of Chemistry College Station, TX 77843			7b ADDRESS (City, State, and ZIP Code) Department of the Navy Arlington, VA 22217	
8a NAME OF FUNDING / SPONSORING ORGANIZATION			9 PROCUREMENT INSTRUMENT IDENTIFICATION NUMBER N00014-79-C-0584	
8b OFFICE SYMBOL (If applicable)			10 SOURCE OF FUNDING NUMBERS	
9c ADDRESS (City, State, and ZIP Code)			PROGRAM ELEMENT NO	PROJECT NO
			TASK NO	WORK UNIT ACCESSION NO
			NRO53-714	
11 TITLE (Include Security Classification) Macrocycles Containing Tin. Solid Complexes of Anions Encrypted in Macrobicyclic Lewis Acid Hosts				
12 PERSONAL AUTHOR(S) Martin Newcomb, John H. Horner, Michael T. Blanda, Philip J. Squattrito				
13a TYPE OF REPORT Technical Report		13b TIME COVERED FROM TO		14 DATE OF REPORT (Year, Month, Day) 1989, Jan 27
15 PAGE COUNT 27				
16 SUPPLEMENTARY NOTATION				
17 COSATI CODES			18 SUBJECT TERMS (Continue on reverse if necessary and identify by block number)	
FIELD	GROUP	SUB-GROUP	tin macrocycle, macrobicycle, complexation, anions, Lewis acid, halide, NMR, X-ray.	
19 ABSTRACT (Continue on reverse if necessary and identify by block number) Crystalline complexes of 1,10-dichloro-1,10-distannabicyclo[8.8.3]hexacosane and benzyltriphenylphosphonium chloride (complex 3) and of 1,8-dichloro-1,8-distannabicyclo[6.6.6]eicosane and tetrabutylammonium fluoride (complex 4) have been studied by X-ray crystallography and solid state ^{119}Sn NMR spectroscopy. The halide ions are encrypted within the cavities of the bicyclic hosts in both complexes. Complex 3 is a stannate-stannane species wherein one of the Lewis acidic tins binds the chloride strongly and the other interacts with the chloride only weakly. Complex 4 is a bis-hemistannate species wherein the Lewis acidic tin atoms bind the guest fluoride simultaneously. Low temperature solution ^{119}Sn NMR spectra of the two complexes in halogenated solvents were studied. A "chloride jump" from one tin to the other was observed in complex 3; the dynamic process has an activation energy of 5.3 kcal/mol. Line broadening of the tin signals in complex 4 was consistent with a similar "fluoride jump" with an activation energy of 2.9 kcal/mol. The crystalline complexes were reasonable models for the solution complexes in both cases, and the structural features in the solid state can be used to rationalize the binding energies in solution.				
20 DISTRIBUTION / AVAILABILITY OF ABSTRACT <input checked="" type="checkbox"/> UNCLASSIFIED / UNLIMITED <input checked="" type="checkbox"/> SAME AS RPT <input type="checkbox"/> DTIC USERS			21 ABSTRACT SECURITY CLASSIFICATION Unclassified	
22a NAME OF RESPONSIBLE INDIVIDUAL			22b TELEPHONE (Include Area Code)	
			22c OFFICE SYMBOL	

OFFICE OF NAVAL RESEARCH

Contract N00014-79-C-0584

R & T Code 413a001-000-01

TECHNICAL REPORT NO. 12



Macrocycles Containing Tin. Solid Complexes of Anions
Encrypted in Macrobicyclic Lewis Acidic Hosts

by

Martin Newcomb, John H. Horner
Michael T. Blanda, Philip J. Squatritto

Department of Chemistry
Texas A&M University
College Station, Texas 77843

January 27, 1989

Prepared for publication in
The Journal of the American Chemical Society

Accession For	
NTIS CPA&I	
DTIC TAB	
Unannounced	
Justification	
By	
Distribution/	
Availability Codes	
Dist	Avail and/or Special
A-1	

Reproduction in whole or in part is permitted for
any purpose of the United States Government

* This document has been approved for public release
and sale; its distribution is unlimited

* This statement should also appear in Item 3 of Document Control Data
- DD Form 1473. Copies of form available from cognizant contract
administrator.

89 1 30 048

**Macrocycles Containing Tin. Solid Complexes of Anions
Encrypted in Macrobicyclic Lewis Acidic Hosts**

Martin Newcomb*, John H. Horner, Michael T. Blanda, Philip J. Squattrito

Department of Chemistry

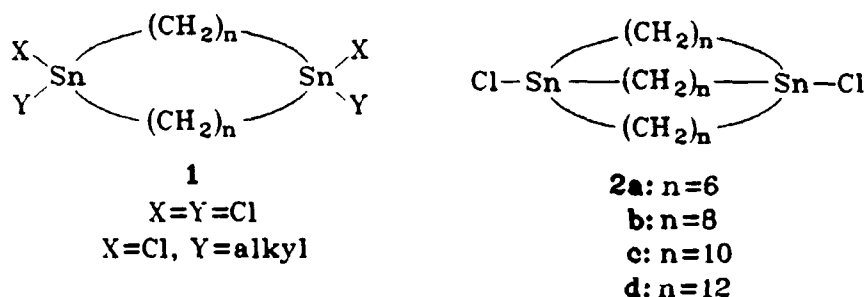
Texas A&M University

College Station, TX 77843

Abstract: Crystalline complexes of 1,10-dichloro-1,10-distannabicyclo[8.8.8]hexacosane and benzyltriphenylphosphonium chloride (complex **3**) and of 1,8-dichloro-1,8-distannabicyclo[6.6.6]eicosane and tetrabutylammonium fluoride (complex **4**) have been studied by X-ray crystallography and solid state ^{119}Sn NMR spectroscopy. The halide ions are encrypted within the cavities of the bicyclic hosts in both complexes. Complex **3** is a stannate-stannane species wherein one of the Lewis acidic tins binds the chloride strongly and the other interacts with the chloride only weakly. Complex **4** is a *bis*-hemistannate species wherein the Lewis acidic tin atoms bind the guest fluoride simultaneously. Low temperature solution ^{119}Sn NMR spectra of the two complexes in halogenated solvents were studied. A "chloride jump" from one tin to the other was observed in complex **3**; the dynamic process has an activation energy of 5.3 kcal/mol. Line broadening of the tin signals in complex **4** was consistent with a similar "fluoride jump" with an activation energy of 2.9 kcal/mol. The crystalline complexes were reasonable models for the solution complexes in both cases, and the structural features in the solid state can be used to rationalize the binding energies in solution.

Macrocycles Containing Tin. Solid Complexes of Anions Encrypted in Macrobicyclic Lewis Acidic Hosts

The host guest chemistry of cation complexation has become a sophisticated field of study, but the corresponding area of guest anion complexation is in a more preliminary state. Studies have shown that charged ammonium ion containing, macrocyclic hosts can bind anions in aqueous solution,^{1,2} and complex Lewis acidic hosts that employ mercury,³ boron,⁴ and silicon⁵ are known that can bind anions in organic solvents. Our group has explored the use of macrocyclic hosts containing Lewis acidic tin atoms for anion complexation in organic media. Macrocycles of various ring sizes containing two or four tin atoms have been described.⁶ However, although anion complexation by hosts like **1** with macrocyclic skeletons was possible, poor selectivity in binding was observed.^{6b} On the other hand, when a third chain was incorporated into the di-tin species to give the more organized macrobicycles **2**, size selective complexation of halides occurred.⁷ Based on the size selective nature of anion binding by hosts **2**, the stoichiometry of the complexes and the greatly reduced rates of complexation and decomplexation by hosts **2** in comparison to simple acyclic and monocyclic analogs, we concluded that the anion was bound within the cavity of the hosts and that the Lewis acidic centers acted in a through space, cooperative manner dictated by the host structure.⁷ This was the predicted behavior of the macrobicycles **2** because it is well known that in simple stannates of structure $R_3SnX_2^-$ the two electron withdrawing groups are in apical positions of the trigonal bipyramid and, thus, hosts **2** contain Lewis acidic binding sites directed into their cavities.



In this work, we report the isolation, solid state studies and low temperature solution NMR studies of two complexes of hosts **2** binding anions, a complex of host **2b** binding the chloride ion (**3**) and one of host **2a** binding the fluoride ion (**4**). X-ray crystallographic studies unequivocally confirmed our expectation that the anions can be encrypted within the host cavities. The two complexes represent extremes in binding with the guest anion isolated on one Lewis acidic site in complex **3** but shared by both acidic tin atoms in complex **4**. Solid state ^{119}Sn NMR spectroscopic studies of the complexes have shown that this technique can provide equally valuable information about the host-guest interactions in the solid. The structural information provided from the solid state studies was useful for modeling the binding interactions in solution.

Chloride Complex 3

Chloride binding studies in solution by the series of hosts **2** gave binding constants that decreased in the order $2b \approx 2c > 2d \gg 2a$.^{7a} The strong binding of chloride by **2b** when host **2a** failed to complex chloride to any measurable extent^{7b} suggested that the cavity in **2b** was close to optimal for this guest. This conclusion was supported by the X-ray crystal structure of free host **2b** which contains a tin-tin distance of 7.56 Å (edge to edge distance of ca 4.8 Å). Because the tin atoms are bound in tetrahedral environments in **2b**, it was anticipated that the tin-tin distance in a complex with trigonal bipyramidal tins could be shorter. The crystal diameter of chloride is ca. 3.6 Å.⁸

Crystalline complexes of simple dichlorotrialkylstannates with the benzyltriphenylphosphonium cation are known.⁹ When host **2b** and one equivalent of benzyltriphenylphosphonium chloride were dissolved in CH₃OH/THF and the mixture was evaporated to dryness, a crystalline complex formed that was recrystallized from acetonitrile. An X-ray crystallographic study of the complex showed that it was a 1:1 complex (**3**). Figure 1 contains ORTEP drawings of the free host **2b** and complex **3**. Table 1 lists some bond angles and lengths for the two structures.

INSERT TABLE 1

As noted, when a halotrialkyltin Lewis acid binds a halide to form a stannate complex, the ligands about tin assume a trigonal bipyramidal geometry with the halides at the apical positions. For example, in the solid state state, the three carbons bonded to tin in dichlorotributylstannate define a plane from which the tin atom is only slightly displaced and the tin chloride bond lengths are 2.57 and 2.68 Å.⁹ Free host **2b** as a solid contains two tetrahedral tin atoms with the Lewis acidic regions of each directed into the cavity. In complex **3**, one of the tin atoms binds the guest chloride strongly (Sn(1)-Cl(2) distance of 2.610(5) Å), and the geometry about this tin atom is essentially trigonal bipyramidal. However, the second tin atom remains in a distorted tetrahedral environment with the Sn(2)-Cl(2) distance of 3.388(5) Å. Thus, complex **3** is a stannate-stannane species. The tin-chlorine bond lengths to the outer chlorides are consistent with this picture; in the "stannate" portion of the complex, the Sn(1)-Cl(1) bond length (2.745(5) Å) is longer than that in the free host, whereas the Sn(2)-Cl(3) bond length in the "stannane" portion of the complex (2.415(5) Å) is quite similar to that in the free host (2.373(3) Å).

The question of how much interaction exists between the bound chloride and the "stannane" tin atom in complex **3** deserves some comment. The stannane portion of complex **3** is a distorted tetrahedron with C-Sn-C bond angles ranging from 114 to 120° and Cl-Sn-C angles ranging from 100 to 103°. This distortion is not, however, significantly greater than that observed in the free host **2b** which has C-Sn-C bond angles between 115 and 117° and Cl-Sn-C angles between 99 and 105°. Thus, from the crystal structure, one concludes that complex **3** is purely a stannate-stannane with no detectable interaction between the chloride inside the cavity and the stannane portion of the complex. However, an interaction was indicated by solid state NMR spectroscopy as discussed below.

The solid state MAS ¹¹⁹Sn NMR spectrum of complex **3** was quite interesting. ¹¹⁹Sn has a large chemical shift anisotropy, and at 7.05 T it is not possible to spin the sample fast enough to eliminate side bands with conventional equipment. Nevertheless, the multi-line spectrum of complex **3** was clearly composed of two signals that were resolved by computer simulation (see Figure 2). The spectrum contains signals at δ -24 and +128 and resembles a composite of the spectra of the free host **2b** and the stannate (Bu₃SnCl₂)⁻ (Figure 3).

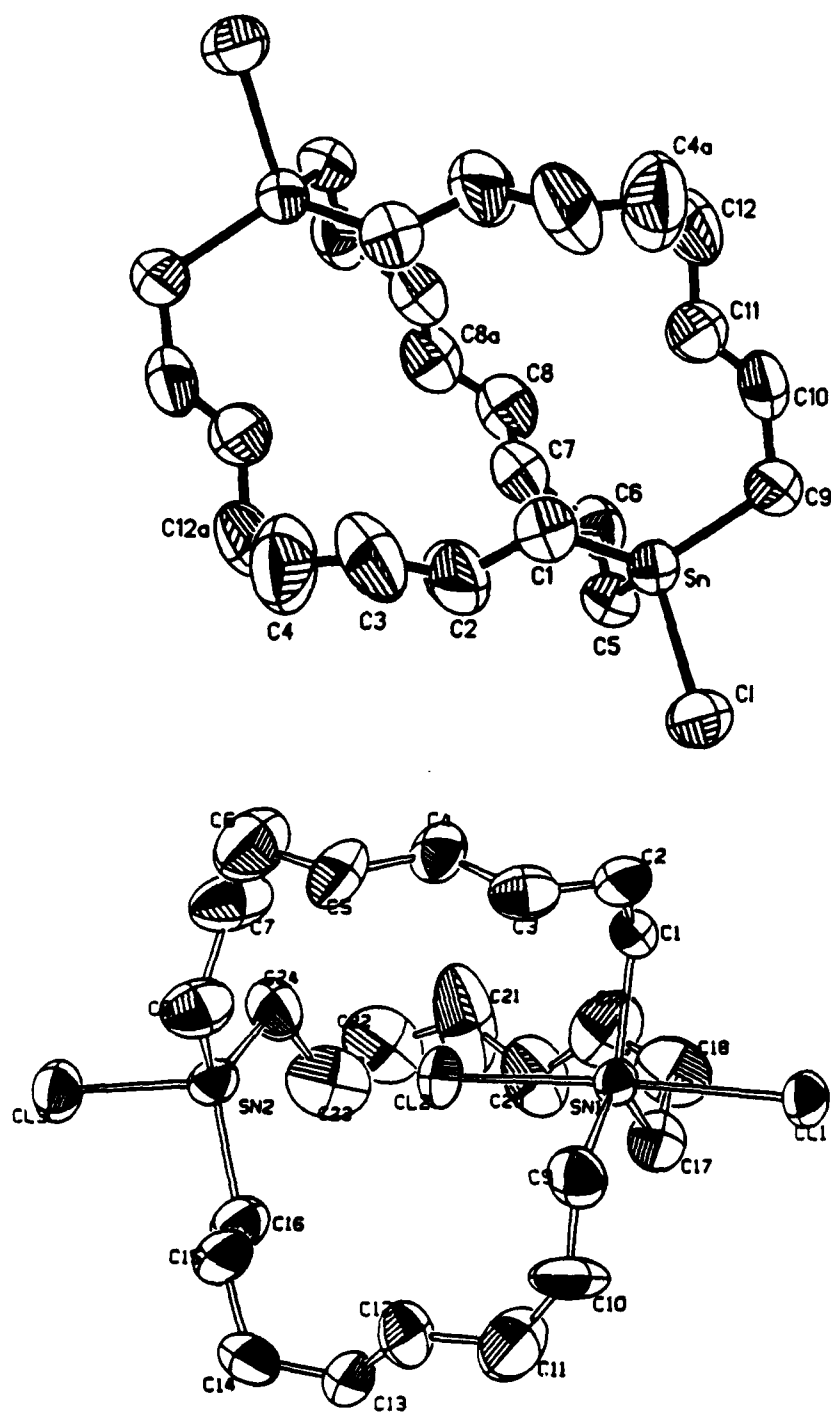


Figure 1. ORTEP drawings of host 2b (top) and the macrocyclic portion of complex 3 (bottom) shown at the 35% probability level. Hydrogen atoms have been omitted.

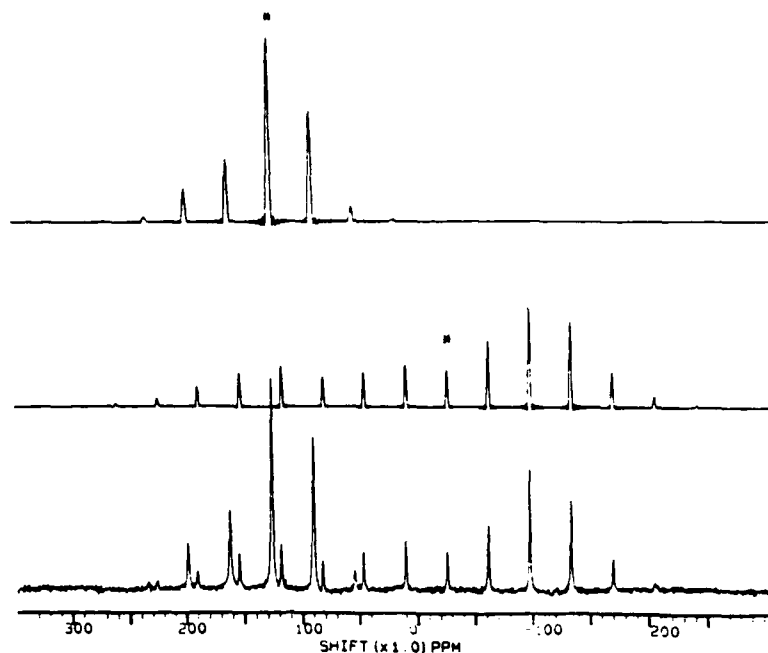


Figure 2. Solid state ^{119}Sn NMR spectra of complex 3. The top trace is a simulation of a signal at δ 128 (starred) with $\eta = 0.43$ and anisotropy = -9.2 kHz. The middle trace is a simulation of a signal at δ -24 (starred) with $\eta = 0.3$ and anisotropy = -28.0 kHz, where $\eta = (\sigma_{yy} - \sigma_{xx})/(\sigma_{zz} - \sigma_0)$ and anisotropy is defined as $\sigma_{zz} - \sigma_0$. The bottom trace is the experimental spectrum of 3 with magic angle spinning at 4 kHz.

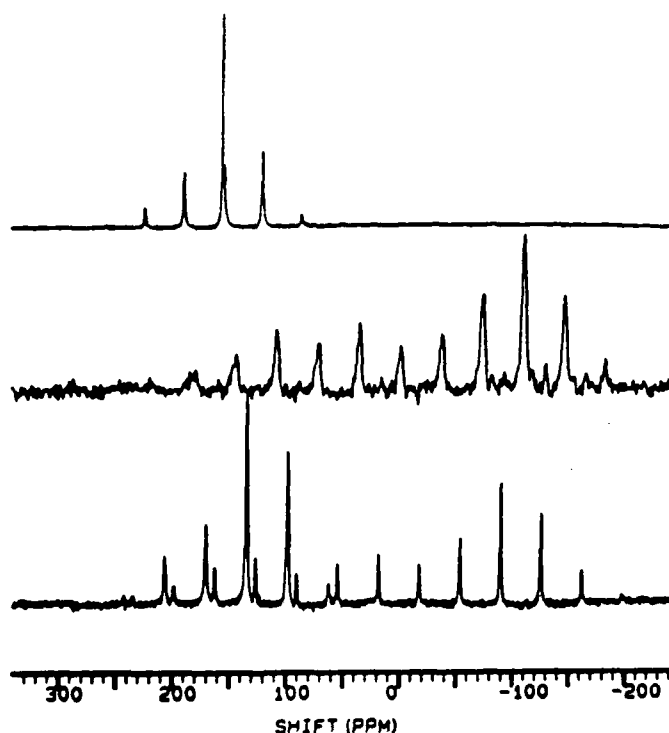


Figure 3. Solid state ^{119}Sn NMR spectra of host 2b (top), the stannate $(\text{Ph}_3\text{PCH}_2\text{Ph})^+ (\text{Bu}_3\text{SnCl}_2)^-$ (middle), and complex 3 (bottom). The spectra were obtained with magic angle spinning at 4 kHz.

In solution ^{119}Sn NMR spectra in simple halogenated solvents, signals from stannate tin atoms of our bicyclic hosts are ca. 200 ppm upfield from those of stannane tin atoms.^{7a,10} Therefore, the upfield signal in the solid state ^{119}Sn NMR spectrum of complex 3 is assigned to the stannate tin and the downfield signal to the stannane tin. The simplicity of the solid state NMR spectrum of 3 shows that this technique can be used to determine details about the structure. Specifically, from only the solid state NMR spectrum it is required that complex 3 contains two distinct tin atoms and it is highly likely that they are "stannane" and "stannate" tin atoms.

^{119}Sn NMR chemical shifts are especially sensitive to the environment about the tin atoms, and the solid state spectrum of complex 3 indicates that there is a weak interaction between the "stannane" tin and the guest chloride. The solid state ^{119}Sn NMR signal for free host 2b at δ 158 and the signal observed for $(\text{Bu}_3\text{SnCl}_2)^-$ at δ -33 are directly analogous to the signals seen in solution in halogenated solvents for these two species (δ 153 for 2b and δ -65¹¹ for $(\text{Bu}_3\text{SnCl}_2)^-$). The chemical shifts observed in the solid state ^{119}Sn NMR spectrum of complex 3 suggest that the guest chloride weakly interacts with the "stannane" tin resulting in a ca. 30 ppm *upfield* shift for this atom. Similarly, the interaction between the guest chloride and the "stannate" tin appears to be slightly weaker than in the acyclic model stannate because this atom gives a signal that is ca. 9 ppm *downfield* from the expected position. If the chemical shifts observed for the tin atoms are directly proportional to the degree of binding with the guest chloride, then this guest is bound ca. 90% to the "stannate" tin and ca. 20% to the "stannane" tin atom, and the complex 3 represents an early stage of dissociation of the guest from the "stannate" tin and the beginning of Lewis acidic binding by the "stannane" tin.

Given the solid state ^{119}Sn NMR spectrum of complex 3, further study of the solution NMR of this interesting complex was warranted. Previously, when complexation of chloride in solution by host 2b was studied by ^{119}Sn NMR spectroscopy in CDCl_3 , dynamic behavior could be observed at temperatures above -50 °C, and line shape analysis was possible.^{7a,10} The dynamic process seen above -50 °C is exchange of free and bound chloride which equilibrates free host 2b (δ +153) with complex 3 (ca δ +27) with an activation energy for the first order decomplexation reaction of 9 to 11 kcal/mol depending upon the solvent and temperature range studied.^{7a,10} At -50 °C, the ^{119}Sn NMR signal for complex 3 was broad, and because of the dynamics of the exchange process, this signal was not found to sharpen at higher temperatures; we simulated the spectrum at -50 °C adequately by ascribing a very short T_2 to the complexed tin signal, but the actual value of T_2 was immaterial for the broad signals seen at higher temperatures.^{7a} The solution ^{119}Sn NMR signal for complex 3 at δ +27 was at about the midpoint of those expected for stannane and stannate tin atoms in CDCl_3 solution; in principle, it could have arisen from either a rapid equilibration of two distinct tin atoms or from two equivalent tin atoms that bound the guest chloride simultaneously.

We have now investigated the solution NMR behavior of 3 in CFCl_3 which permits studies at lower temperatures. The ^{119}Sn NMR spectrum at -20 °C of a 0.02 M solution of 2b and a 5-fold excess of tetrahexylammonium chloride in CFCl_3 showed a single sharp line at ca δ +8. Upon cooling, this signal broadened steadily, and, at -100 °C, an extremely broad signal obviously near coalescence was observed (Figure 4). It would appear to be clear that the dynamic phenomena seen at these low temperatures is the "chloride jump" from one tin atom to the other in complex 3. Simulations of the low temperature solution ^{119}Sn NMR spectra of 3 were possible; however, since we were unable to slow the exchange process

enough to determine experimentally the limiting values for the two tin atoms in solution, it was necessary to estimate the chemical shifts of these atoms. In the solid state ^{119}Sn NMR spectrum of 3, the $\Delta\delta$ between the two tin atoms was 143 ppm, and this is probably a reasonable value for $\Delta\delta$ in solution. Alternatively, the $\Delta\delta$ value might be as large as 265 ppm which is twice the difference between the chemical shifts of free 2b and complex 3. Simulations were performed using 140 and 265 ppm as the likely extremes for the stannane-stannate difference in 3, and the results are given in Table 2. The choice of the $\Delta\delta$ value slightly affects the kinetic values, but does not significantly affect the activation energy obtained from these values as long as $\Delta\delta$ does not change with temperature. The kinetic values calculated for $\delta\Delta = 140$ ppm gave a better fit in an Arrhenius treatment. Using the values from $\delta\Delta = 140$ ppm, the "chloride jump" has an activation energy of only 5.3 kcal/mol; the dynamic phenomena is described by eq 1 where the errors are 1σ and $\theta = 2.3 \text{ RT kcal/mol}$.

$$\log(k_{\text{ex}}/\text{s}^{-1}) = (11.9 \pm 0.2) - (5.3 \pm 0.2)/\theta \quad (1)$$

INSERT TABLE 2

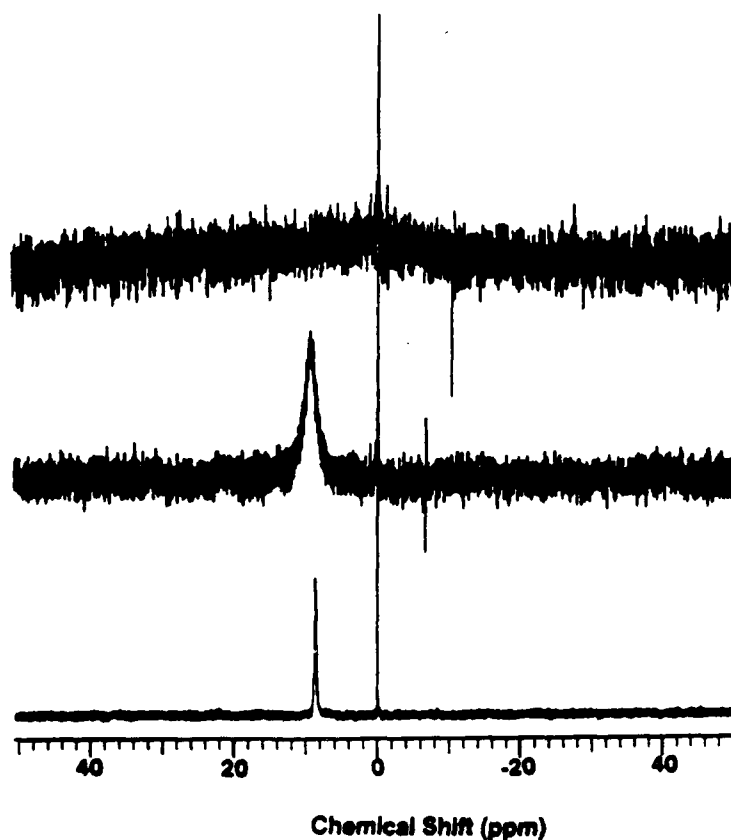


Figure 4. Solution ^{119}Sn NMR spectra of complex 3 in CFCl_3 at -100 (top), -60 (middle) and -20 $^\circ\text{C}$ (bottom). The signal at δ 8 is from the complex; the sharp signal at δ 0 from internal Me_4Sn is truncated.

Fluoride Complex 4

Host **2a** appears not to be a Lewis acid for any anion except fluoride, but **2a** binds fluoride strongly.^{7b} When solutions of $\text{Bu}_4\text{N}^+\text{F}^-$ and host **2a** were studied by solution ^{119}Sn NMR spectroscopy, we observed a signal as a doublet at $\delta -6.5$ with a ^{19}F coupling constant of ca 1100 Hz. Because of the highly selective nature of binding exhibited by **2a**, we concluded that F^- was bound within the cavity of the host.^{7b} The chemical shift for the complexed tin signal was at the midpoint of those expected for a stannane and a stannate tin atom, and, at temperatures above -20°C , we could not differentiate between structures wherein the F^- was held simultaneously by the tins or rapidly exchanged between the tins. An X-ray crystal structure of free host **2a** showed that the distance between the tin atoms was 5.25 Å (edge to edge distance of about 2.45 Å), and this distance was expected to be smaller in the complex with trigonal bipyramidal tin atoms. It was possible that both tin atoms bound the F^- (crystal diameter of 2.6 Å)⁸ simultaneously.

When a solution of $\text{Bu}_4\text{N}^+\text{F}^-$ and host **2a** in THF was cooled, a crystalline complex formed. Dissolution of the complex in CDCl_3 and ^{13}C NMR spectroscopy suggested that the complex had 1:1 stoichiometry. An X-ray crystallographic study showed that the species was a 1:1 complex (**4**). Figure 5 contains ORTEP drawings of free host **2a** and complex **4**. Table 3 contains representative bond angles and lengths for the two structures.

INSERT TABLE 3

Unlike chloride complex **3**, fluoride complex **4** has a nearly symmetrical structure. Both tin atoms are bound to the fluoride; the Sn-F bond lengths are essentially equal (2.12(4) and 2.28(4) Å). The Sn-Cl bond lengths in the complex (2.66(1) and 2.57(1) Å) are somewhat longer than those in the free host **2a** (2.36(2) and 2.39(2) Å). It is noteworthy that these Sn-Cl bonds are not as long as the Sn(1)-Cl(1) bond, the stannate bond, in complex **3**. The tin atoms in complex **4** are in distorted trigonal bipyramidal environments with the central tin atoms located ca 0.047 and 0.055 Å from the planes defined by their three α -carbons. The Sn-Sn distance in complex **4** is reduced to 4.40 Å. Thus, in the solid state, complex **4** has a *bis*-hemistannate structure rather than the stannane-stannate structure of complex **3**.

Complex **4** was also studied by MAS solid state ^{119}Sn NMR spectroscopy. Only one type of tin atom was found; the signal was a doublet centered at $\delta -50$ with an F^- coupling constant of 1120 Hz. As in the case of complex **3**, the solid state ^{119}Sn NMR spectrum contains adequate information to assign a tentative structure to the complex.

We can ask if the solid state structure of complex **4** describes the complex in solution. Previously, the solution ^{119}Sn NMR spectrum of **4** could be observed from a mixture of **2a** and $\text{Bu}_4\text{N}^+\text{F}^-$.^{7b} The same ^{119}Sn NMR spectrum was observed when crystalline complex **4** was dissolved in CDCl_3 . The complex was in the slow exchange limit, and the signal from free host was observed at $\delta 148$ with no line broadening. The solution spectra contained a sharp doublet centered at $\delta -6.5$ ($J = 1100$ Hz) for the complex. When spectra of an 0.1 M solution of **4** in CDCl_3 were studied over the temperature range 0 to -50°C , we observed an increasing line broadening for the complex signals. This broadening might have arisen from a rapid exchange between two nonequivalent tin sites (a fluoride jump) or some other combination of relaxation processes not dominated by exchange.

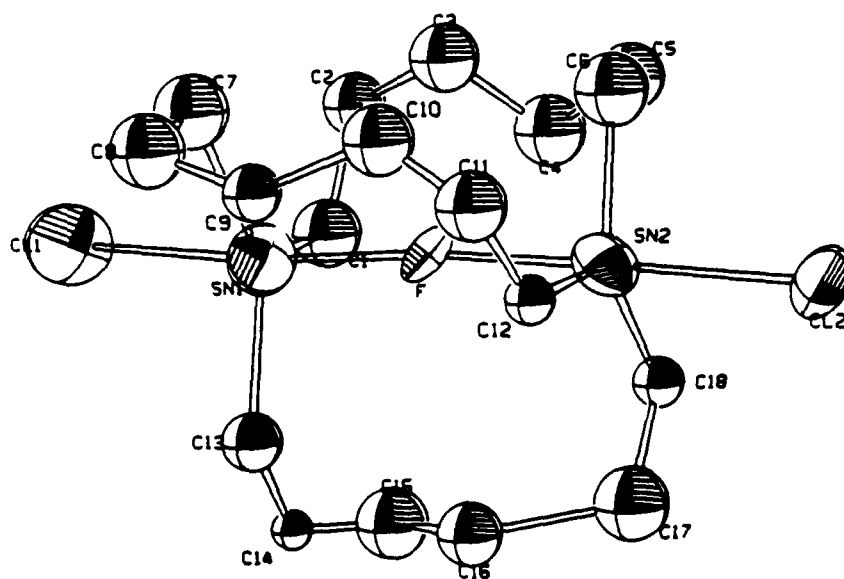
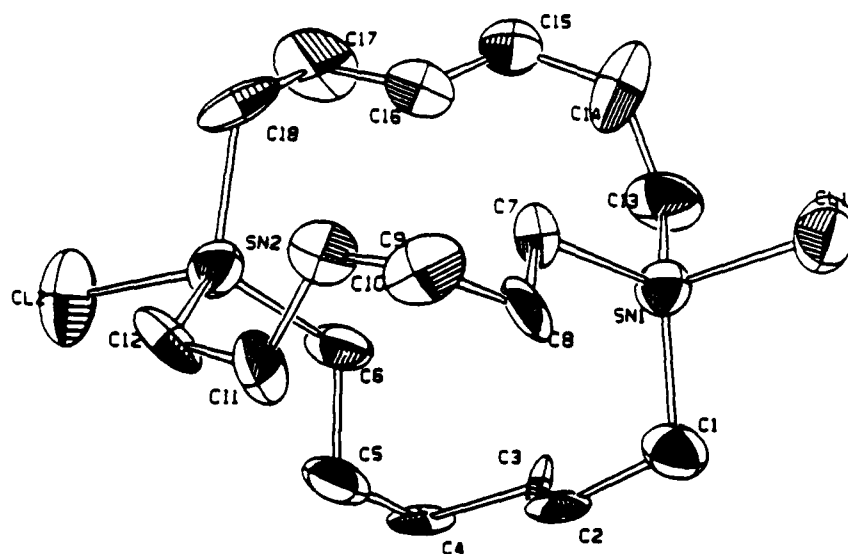


Figure 5. ORTEP drawings of host **2a** (top) and the macrocyclic portion of complex **4** (bottom) shown at the 35% probability level. Hydrogen atoms have been omitted.

An attempt was made to elucidate the origin of the line broadening of the signal from complex 4 (which requires a T_2 of ca. 1×10^{-4} s at -50°C) by examining the potential effects from different sources, and all contributors to T_2 except exchange were judged to be insignificant.¹² The possibility that the transverse relaxation of the complex was dominated by a dynamic exchange was further explored by fixing the other contributors to T_2 at 0.05 seconds (the value measured for host 2b) and simulating the spectra with a two site exchange model. The resulting kinetic values were then used to determine if the apparent activation energy and log A for the purported exchange process were reasonable. Simulations were performed on extreme cases where the $\Delta\delta$ values for the two sites were 45,000 Hz and 300 Hz; Table 4 contains the results. The rate constants varied by two orders of magnitude for the two cases, but the Arrhenius plots gave similar values for E_a (2.5 and 2.9 kcal/mol, respectively) that were not unreasonable. Thus, we conclude that an exchange process was occurring in solution and that the exchanging sites were located within several hundred Hz of one another. This structural picture of the complex in solution is consistent with the solid state structure because the X-ray results showed two distinct (albeit quite similar) tin atoms and the resolution in the solid state ^{119}Sn NMR spectrum was too poor to permit the observation of two signals varying in chemical shifts by only a few hundred Hz (the line widths in the solid state NMR spectrum were ca 1000 Hz at the base).

INSERT TABLE 4

Complex Structures and Binding Constants in Solution

The solid state structures of complexes 3 and 4 show that hosts 2a and 2b bind their respective anionic guests in dramatically different fashions, and the solid state structures apparently are good models for binding in solution. Thus, it was of interest to determine how the different binding modes affected the equilibrium constants for binding in solution.

Binding constants for host 2b complexing chloride in solution were previously determined by dynamic NMR studies.^{7a,10} In $\text{C}_2\text{D}_2\text{Cl}_4$ solution at 30°C , host 2b binds chloride with an equilibrium constant of 7 M^{-1} . For comparison, we have determined the binding constant for chloride by the simple acyclic model tributyltin chloride (5). Model 5 binds chloride in fast exchange at all temperatures, so the NMR spectra of a mixture of 5 and chloride contain only one signal. The equilibrium constant for 5 binding chloride could be calculated by an iterative Hildebrand-Benesi treatment; in CDCl_3 solution at 20°C , the binding constant is ca 17 M^{-1} . Despite the presence of two Lewis acidic sites in host 2b, the chloride binding constant for 2b is slightly less than that of the simple mono-tin model 5. Apparently, this reflects the fact that 2b only binds chloride effectively with one of its acidic sites, and any increased binding energy resulting from a simple statistical effect of the two tin atoms in the host might be offset by the non-polar nature of the hydrocarbon linking chains. Thus, size selective binding of chloride by 2b results almost entirely from the size of the cavity.

The situation appears to be different for host 2a binding fluoride. Previously, we calculated a conservative estimate of the binding constant for complexation of fluoride by 2a.^{7b} Now, with crystalline complex 4 with an exact 1:1 stoichiometry for the host and fluoride ion in hand, we have been able to obtain more accurate binding constants for complex formation in solution even though rate constants were too slow to measure. Strong binding was observed from -50 to 30°C in CDCl_3 and $\text{C}_2\text{D}_2\text{Cl}_4$ solutions with binding constants on the order of $1\text{--}2 \times 10^4 \text{ M}^{-1}$. Unfortunately, there is no simple model compound

analogous to complex 4 because the halide ligands on simple tin species exchange rapidly and it is not possible to observe a stannate that has two different halide ions. The binding constant for Bu_3SnF binding F^- in CDCl_3 was determined by a Hildebrand-Benesi treatment ($K < 10 \text{ M}^{-1}$), but this is a poor model because Bu_3SnF self aggregates strongly in solution. When F^- was added to a CDCl_3 solution of Bu_3SnCl at 30°C , the apparent binding constant was about 200 M^{-1} , but a mixture of rapidly exchanging tin species were present in this study. Despite the lack of a good model, it appears to be clear that host 2a binds fluoride substantially more strongly than would be expected for a simple acycle. The increase in the binding constant for 2a probably results from the fact that the acidic tin atoms bind the fluoride simultaneously.

Thus, the binding constants for hosts 2a and 2b are strongly dependent on the nature of the complex. Host 2b binds chloride selectively mainly because of the cavity size excludes some ions and the structure may permit a small statistical effect from two Lewis acidic sites. On the other hand, for host 2a, where the guest fluoride fits precisely in the cavity and is bound in a true bidentate manner, a substantial increase in binding energy is apparent.

Conclusion

A few crystalline complexes containing halide ions bound within a macropolycyclic host have been obtained previously.^{2,14} However, in these cases the host contained protonated or quaternized nitrogen atoms, and the origin of the binding was of an electrostatic, charge-charge nature. The complexes reported here represent examples of halides encrypted within a highly structured host and held by dative, Lewis acid-base bonds. The crystal structures of complexes 3 and 4 display some unique features. The *bis*-hemistannate structure in complex 4 is highly unusual. Perhaps complex 3 has an even more novel structure in that it contains a chloride anion bound to a Lewis acid in an early stage of dissociation and, at the same time, a Lewis acidic site in an early stage of accepting a donor.

For the cases studied in this work, the crystal structures appear to be good models for the corresponding bound species in solution. Thus, the detailed information provided by X-ray crystallography can be used to understand the details of solution binding. Solid state NMR spectroscopy, while less informative than X-ray crystallography, can also provide information for solution binding, and the relative simplicity of this method makes it especially attractive.

Experimental Section

General. All reagents were obtained from Aldrich Chemical Company; benzytriphenylphosphonium chloride was dried under vacuum (ca 0.1 Torr) at 25°C for at least 24 h before use, the remainder of the reagents were used as received. Solution NMR spectra were obtained on a Varian XL-400 or a Varian XL-200 spectrometer. Solid state NMR spectra were obtained on a Bruker MSL-300 spectrometer. X-ray structural measurements were made on Rigaku AFC5R and Nicolet R3m/V diffractometers.

The syntheses of bicyclic hosts 2a and 2b have been reported.^{7a,10}

Complex 3. Bicyclic 2a (0.526 g, 0.816 mmol) and benzytriphenylphosphonium chloride (0.321 g, 0.825 mmol) were dissolved in a THF/methanol mixture. The solvent was removed under vacuum, and the resulting white precipitate was recrystallized from acetonitrile to give 3 as a white solid (0.67 g, 80%) with mp $197\text{--}200^\circ\text{C}$.

Complex 4. To a solution of 300 mg (0.54 mmol) of **2a** in 10 mL of dry THF was added 0.6 mL of a 1 M solution of tetrabutylammonium fluoride in THF. A solid crystallized from solution over several hours at room temperature. The solid was collected by filtration and washed with small portions of cold THF. The isolated yield of white, crystalline product **4** was 330 mg (0.39 mmol, 75%). The complex had mp > 220 °C. Solution NMR spectra in CDCl₃ (¹H NMR at 200 MHz, ¹³C NMR at 50 MHz) contained the signals from **2a**⁷ and the salt.

Benzyltriphenylphosphonium dichlorotributylstannate was prepared by the reported procedure.⁹ The crystalline complex was obtained in 89% yield and had mp 92-94 °C (lit.⁹ mp 115-118 °C).

Solid State ¹¹⁹Sn NMR spectra were obtained at 111.9 MHz. Magic angle spinning and proton-tin cross polarization were employed. Samples were spun at 2.5 to 4 KHz. Spectra were recorded at 20 °C. External Me₄Sn (δ = 0) was used as the standard. The chemical shifts of the multi-line spectra were determined by computer simulation¹⁵ or by comparison of spectra recorded at slightly different spinning rates. ¹¹⁹Sn chemical shifts for the various species were as follows: **2a**, 148; **2b**, 158; **3**, 128, -24; **4**, -50 (d, J = 1120 Hz); [Ph₃PCH₂Ph]⁺ [Bu₃SnCl₂]⁻, -33.

Low temperature solution NMR spectra were measured on a Varian XL-400 at 149 MHz. Temperatures are believed to be accurate to better than ±1 °C. For studies of the exchange of chloride within the cavity of host **2b**, a CFC₃ solution containing 0.02 M **2b** and 0.1 M tetrahexylammonium chloride was employed. For studies of the exchange of fluoride within the cavity of host **2a**, a CDCl₃ solution containing 0.1 M **4** was employed. The spectra were simulated with a two-site exchange program based on a published method.¹⁶

Binding constants in solution. The equilibrium constants for host **2b** binding chloride ion in CDCl₃ and C₂D₂Cl₄ have been reported.^{7a,10}

The equilibrium constants for host **2a** binding fluoride ion were determined. Solutions of complex **4** in CDCl₃ (0.064 M) and in C₂D₂Cl₄ (0.064 M) were prepared. ¹¹⁹Sn NMR spectra were recorded at various temperatures. Slow exchange between free host (δ 148) and complex (δ -6.5, d, J = 1100 Hz) was observed at all temperatures. The ratio of free host to complex was determined by direct integration of the signals. (Care was taken to ensure that the transmitter was located at the midpoint of the two signals to guarantee that each signal received equal power.) Free fluoride was taken to be equal to free host, and the equilibrium constants for binding were solved directly from eq 2 where K is the equilibrium constant for formation of the complex, C is the complex, H is free host and F is free fluoride. Over the temperature range -50 to 30 °C, K appeared to be insensitive to temperature giving values that ranged from 6000 to 22,000 M⁻¹ with no substantial systematic temperature dependent deviation; the large range of values for K resulted from errors in measuring the small amount (2-3%) of free host and fluoride present under these conditions.

$$K = [C]/([H][F]) = [C]/[H]^2 \quad (2)$$

Five solutions of tributyltin chloride (**5**) in CDCl₃ (0.02 M) were prepared. Tetrahexylammonium chloride was added to each to give solutions ranging from 0.05 to 0.30 M in chloride. ¹¹⁹Sn NMR spectra were recorded at 50, 20, -20 and -50 °C. One sharp signal was observed in all cases. The binding constants were determined by a modified double reciprocal treatment (Hildebrand-Benesi method¹⁷) wherein the value of K was determined and the concentrations of free chloride were recalculated; the procedure was repeated until the results converged.

The equilibrium constant for tributyltin fluoride binding fluoride was determined by the procedure described above for 5. A solution containing 0.4 M tributyltin fluoride was prepared and aliquots of tetraethylammonium fluoride were added. ^{119}Sn NMR spectra were recorded at 20 °C. One broad signal was observed in all cases.

The apparent equilibrium constants for 5 binding fluoride have been reported.^{7b}

X-ray crystal structures for 2b, 3, 2a and 4 were determined. Experimental details follow. Selected bond distances and angles for each are given in Tables 1 and 3. Cell parameters and other relevant crystallographic details are given in Table 5. Final positional parameters and isotropic thermal parameters for the non-hydrogen atoms for the tin species are given in Tables 6-9. Anisotropic thermal parameters, structure amplitudes, hydrogen atom positions, and parameters for the counterions in 3 and 4 are included in the supplementary material.

INSERT TABLES 5-9

$\text{Sn}_2\text{Cl}_2(\text{C}_8\text{H}_{16})_3$ (2b). A colorless crystal of 2b [0.12 mm x 0.24 mm x 0.36 mm] was mounted on a glass fiber at room temperature. Preliminary examination and data collection was performed on a Nicolet R3/m diffractometer [oriented graphite crystal monochromator; $\text{Mo}(\text{K}\alpha = 0.71073 \text{ \AA})$ radiation, operating at 1925 Watts]. Cell parameters were calculated from the least-squares fitting of the setting angles for 25 reflections. Omega scans of several intense reflections indicated acceptable crystal quality. Data were collected at 296(1) K with the $\theta - 2\theta$ technique in the ranges $-21 \leq h \leq 21$, $-15 \leq k \leq 0$, $-15 \leq l \leq 0$. The scan range for 2b for data collection was 1.20° plus $\text{K}\alpha$ separation, with a variable scan rate of 2.03 to $29.30^\circ/\text{min}$. Three control reflections, collected every 97 reflections, showed no significant trends. Backgrounds were measured by a stationary crystal and stationary counter technique at the beginning and end of each scan for one-half the total scan time. A semi-empirical absorption correction (ψ -scan method) was applied to the data set. Reflection intensities were profiled employing a learnt profile technique.¹⁸ The structure was solved by direct methods (SHELXS).¹⁹ All non-hydrogen atoms were refined anisotropically. Hydrogen atoms were placed in idealized positions and included as fixed contributors to F_c . The final refinement of the structure was performed with the use of the TEXSAN²⁰ series of programs as described below for 2a.

Irregular bond distances and angles for some of the carbon atoms were noted. These may be due to unresolved positional disorder caused by closely related conformations of the C_8 chains.

$\text{Sn}_2\text{Cl}_2(\text{C}_8\text{H}_{12})_3$ (2a). Lattice parameters were determined at 298 K from the setting angles of 21 reflections in the range $30^\circ < 2\theta(\text{MoK}\alpha_1) < 36^\circ$ accurately centered on a Rigaku AFC5R diffractometer equipped with a 12 kW rotating anode Mo source. Intensity data were collected at room temperature with the $\omega - 2\theta$ scan technique. Weak data were rescanned up to two additional times. Three standard reflections monitored at 150 reflection intervals experienced intensity drop-offs of 3-5% which were not deemed significant enough to warrant applying a decay correction to the data set. An empirical absorption correction employing the ψ -scan method was applied to the data.

All calculations were performed with the use of the TEXSAN²⁰ series of programs on a Digital Equipment Corp. MicroVAX II computer. The systematic absences ($h0l$, $h + l \neq 2n$) are characteristic of the space groups $\text{P}2_1/\text{n}$ and Pn . The non-centrosymmetric group Pn was chosen because it alone could accommodate an ordered arrangement of the Sn atoms in positions having the required site symmetry (1) for an atom coordinated to three C atoms and one Cl atom in a tetrahedral arrangement. The Sn atoms

were located from a Patterson map while the Cl and C atoms were found by direct methods (DIRDIF²¹). The positions of the H atoms were idealized (C-H = 0.95 Å) and included as fixed contributions to F_o in the final calculations. In order to maximize the observation to variable ratio, the final refinement, which included anisotropic thermal parameters for all non-hydrogen atoms, was performed using all 1968 unique F_o^2 values. The final agreement indices on F_o^2 are given in Table 5. The conventional R index for the 1151 data with $F_o^2 > 3\sigma(F_o^2)$ is 0.033. An analysis of F_o^2 vs F_c^2 as a function of F_o^2 , $\sin \theta/\lambda$, and Miller indices displays no unusual trends. The final difference electron density map was featureless.

The irregular bond distances and angles of some of the carbon atoms may be due to an unresolved positional disorder involving closely related conformations of the C_6 chains. We note that the torsional angles for both the gauche (48(4)° - 70(4)°) and the anti (168(2)° - 175(3)°) interactions are somewhat distorted from the ideal values.

[Sn₂Cl₂(C₈H₁₆)₃ · Cl][(C₆H₅)₃(C₆H₅CH₂)P] (3). Lattice parameters were determined as for 2a from 22 reflections in the range 24° < 2θ(MoKα₁) < 28°. Data were collected at room temperature with the use of ω-scans and Lehmann-Larsen processing.²² This method was selected because of the generally poor diffraction of the crystal. Small (2-8%) decreases in the intensity of 3 standard reflections were noted, however the data were not corrected for either decay or absorption ($\mu = 12 \text{ cm}^{-1}$).

Crystallographic computing was performed as for 2a. The systematic absences ($h0l, h+l \neq 2n; 0k0, k \neq 2n$) are consistent with space group P2₁/n. The Sn atoms were found on an E-map generated by the program MITHRIL²³. The Cl, P, and some of the C atoms were located by direct methods (DIRDIF²¹), while the rest of the C atoms were revealed in difference electron density maps. The positions of the hydrogen atoms were idealized (C-H = 0.95 Å) and included in the model as fixed contributors to F_c . Due to the limited number of observed ($I > 3\sigma(I)$) data, the benzyltriphenylphosphonium cation was refined isotropically, except for the P atom. The final refinement was performed on the 2182 unique F_o values with $I > 3\sigma(I)$ and included anisotropic thermal parameters for the Sn, Cl, and P atoms and all the C atoms in the [Sn₂Cl₂(C₈H₁₆)₃ · Cl] anion, and isotropic thermal parameters for the C atoms in the [(C₆H₅)₃(C₆H₅CH₂)P] cation. The final R values are listed in Table 5. The final difference Fourier map and F_o vs F_c analysis were unexceptional.

[Sn₂Cl₂(C₆H₁₂)₃ · F][(C₄H₉)₄N] (4). Lattice parameters were determined as for 2a from the setting angles of 20 reflections (8° < 2θ(MoKα₁) < 15°). Data were collected at room temperature with the use of the ω-scan technique. Due to the weakly diffracting nature of the crystal (i.e., low signal-to-noise for most peaks), a Lehmann-Larsen profile analysis²² was applied to each of the data in an attempt to maximize the number observed. Even so, as indicated in Table 5, the number of observed data is small compared to the total number measured. Three standards, measured at 150 reflection intervals, showed small intensity losses (3-7%) from beginning to end of data collection. The data were not corrected for decay or absorption ($\mu = 14 \text{ cm}^{-1}$).

All calculations were performed as for 2a. The systematic absences ($h0l, h \neq 2n$) are indicative of the space groups Pa and P2/a. As the Sn atoms could only be accommodated in the non-centrosymmetric group Pa, this group was selected and is accepted on the basis of the successful structure solution obtained. The structure was solved by direct methods: the Sn atom positions were taken from an E map (MITHRIL²³) while the Cl, F, N, and C atoms were located by successive phase refinements with the use of the program DIRDIF.²¹ Due to the limited number of observed data and the poor quality of

the many weak data, refinement of a full anisotropic model was not possible. Consequently, the final refinement performed on the 681 unique F_o values for which $I > 3\sigma(I)$ included anisotropic thermal parameters for the Sn, Cl, F, and N atoms and isotropic thermal parameters for all C atoms. Owing to some rather large distortions in the carbon chains, particularly in the tetrabutylammonium cation, hydrogen atom positions were not included in the model. The final residuals are given in Table 5. No unusual trends in F_o vs F_c appear as a function of F_o , $\sin \theta/\lambda$, or Miller indices. There were no significant peaks in the final difference electron density map.

Acknowledgment. This work was supported by the Office of Naval Research. PJS acknowledges support from the Robert A. Welch Foundation. The Rigaku AFC5R diffractometer was obtained under DOD contract No. N-00014-86-G-0194. The Nicolet R3m/V diffractometer was obtained with funds provided by the National Science Foundation (CHE-8513273). We thank Dr. J. H. Reibenspies for determining the structure of 2b and Dr. P.-J. Chu for the solid state NMR spectroscopic measurements and the simulations of the solid state spectra. We thank Professor A. Clearfield for helpful discussions.

Supplementary Material Available: Tables containing anisotropic thermal parameters, structure amplitudes, final positional parameters and isotropic thermal parameters for the non-hydrogen atoms for the counterions in 3 and 4, and hydrogen atom positions for structures 2b, 3, 2a and 4 (123 pages).

References and Notes

1. Simmons, H. E.; Park, C. H. *J. Am. Chem. Soc.* **1968**, *90*, 2428-2429; 2429-2431; 2431-2432. Schmidtchen, F. P. *Angew. Chem., Int. Ed. Engl.* **1977**, *16*, 720-721.
2. Jazwinski, J.; Blacker, A. J.; Lehn, J.-M.; Cesario, M.; Guilhem, J.; Pascard, C. *Tetrahedron Lett.* **1987**, *28*, 6057-6060. Jazwinski, J.; Lehn, J.-M.; Mric, R.; Vigneron, J.-P.; Cesario, M.; Guilhem, J.; Pascard, C. *Tetrahedron Lett.* **1987**, *28*, 3489-3492. Graf, E.; Lehn, J.-M. *J. Am. Chem. Soc.* **1976**, *98*, 6403-6405. Dietrich, B.; Guilhem, J.; Lehn, J.-M.; Pascard, C.; Sonveaux, E. *Helv. Chim. Acta* **1984**, *67*, 91-104. Hosseini, M. W.; Lehn, J.-M. *Helv. Chim. Acta* **1986**, *69*, 587-603.
3. Wuest, J. D.; Zacharie, B. *J. Am. Chem. Soc.* **1987**, *109*, 4714-4715. Beauchamp, A. L.; Olivier, M. J.; Wuest, J. D.; Zacharie, B. *Organometallics* **1987**, *6*, 153-156. Beauchamp, A. L.; Olivier, M. J.; Wuest, J. D.; Zacharie, B. *J. Am. Chem. Soc.* **1986**, *108*, 73-77. Wuest, J. D.; Zacharie, B. *Organometallics* **1985**, *4*, 410-411.
4. Katz, H. E. *Organometallics* **1987**, *6*, 1134-1136. Katz, H. E. *J. Am. Chem. Soc.* **1986**, *108*, 7640-7645. Katz, H. E. *J. Org. Chem.* **1985**, *50*, 5027-5032.
5. Jung, M. E. *Tetrahedron Lett.* **1988**, *29*, 297-300.
6. (a) Azuma, Y.; Newcomb, M. *Organometallics* **1984**, *3*, 9-14. (b) Newcomb, M.; Madonik, A. M.; Blanda, M. T.; Judice, J. K. *Organometallics* **1987**, *6*, 145-150.
7. (a) Newcomb, M.; Horner, J. H.; Blanda, M. T. *J. Am. Chem. Soc.* **1987**, *109*, 7878-7879. (b) Newcomb, M.; Blanda, M. T. *Tetrahedron Lett.* **1988**, *29*, 4261-4264.
8. Cotton, F. A.; Wilkinson, G. *Advanced Inorganic Chemistry*, 3rd edition; Wiley: New York, 1972, p. 458.
9. Harrison, P. G.; Molloy, K.; Phillips, R. C.; Smith, P. J. *J. Organomet. Chem.* **1978**, *160*, 421-434.

10. Horner, J. H.; Blanda, M. T.; Newcomb, M. submitted for publication.
11. This chemical shift is the value that results from a Hildebrand-Benesi treatment of NMR data for mixtures of Bu_3SnCl and chloride ion at 20 °C. The chemical shift is highly temperature dependent and varies from $\delta -112$ at 50 °C to $\delta -36$ at -50 °C.
12. Because the signal from free host **2a** remained sharp at all temperatures, viscosity effects could not be the origin of the line broadening. ^{13}C NMR spectra of the complex were measured at +20 and -50 °C, and a standard algorithm was used to determine the T_1 values of 0.32 and 0.14 s at the two respective temperatures. From the T_1 values, the correlation time (t_c) for the complex was calculated to be 2.2×10^{-10} s at -50 °C.¹³ This value leads to an estimate of the radius of the species of about 7 Å, and, thus, aggregation of the complex to give large species was not the origin of the line broadening. Other contributors to T_2 could be estimated from the t_c value;¹³ the contribution from dipole-dipole interactions was calculated to be 2 to 2.2 s, and the contribution from shielding anisotropy was estimated to be 2 s. The T_2 contribution from spin rotation was estimated to be greater than 10 s. The scalar coupling contribution to T_2 could be as small as 0.003 s at -50 °C, but this effect, while it probably is the major contributor to T_2 in our non-exchanging systems, could not be the origin of the line broadening we observed since the scalar coupling contribution to T_2 increases as the temperature decreases which would lead to sharper lines at lower temperatures.
13. Harris, R. K. *Nuclear Magnetic Resonance Spectroscopy: A Physicochemical View*; Longman: London, 1986. Farrar, T. C. *An Introduction to Pulse NMR Spectroscopy*; Farragut Press: Chicago, 1987.
14. Bell, R. A.; Christoph, G. G.; Fromzeck, R. R.; Marsh, R. E. *Science* **1975**, *190*, 151-152. Metz, B.; Rosalky, J. M.; Weiss, R. *J. Chem. Soc., Chem. Commun.* **1976**, 533-534. Müller, G.; Schmidtchen, F. P. *J. Chem. Soc., Chem. Commun.* **1984**, 1115-1116.
15. The solid state NMR spectral simulations were obtained with a program written by Dr. P.-J. Chu; Chu, P.-J. unpublished results.
16. Sandström, J. *Dynamic NMR Spectroscopy*; Academic: London, 1982.
17. See Connors, K. A. *Binding Constants, The Measurement of Molecular Complex Stability*; Wiley-Interscience: New York, 1987.
18. Diamond, R. *Acta Crystallogr.* **1969**, *A25*, 43-55.
19. SHELXTL PLUS program package, Sheldrick, G. M.; supplied by Nicolet XRD Corp.
20. TEXSAN, *Texray Structural Analysis Package*; Molecular Structure Corporation: The Woodlands, Texas, 1987 (revised).
21. Beurskens, P. T. *DIRDIF: Direct Methods for Difference Structures--An Automatic Procedure for Phase Extension and Refinement of Difference Structure Factors*. Technical Report 1984/1. Crystallography Laboratory, Toernooiveld, The Netherlands.
22. MSC/AFC Diffractometer Control Software; Molecular Structure Corporation: The Woodlands, Texas, 1988 (revised).
23. Gilmore, C. J. In *Computational Crystallography*; Sayre, D., Ed.; Oxford University Press: London, 1982, pp 176-190.

Table 1. Selected Interatomic Distances and Bond Angles for Host **2b** and Complex **3**.

Interatomic Distances (Å) in Host 2b			
Sn-Cl	2.373 (3)	Sn-C(1)	2.12 (1)
Sn-C(5)	2.08 (2)	Sn-C(9)	2.11 (1)
Sn-Sn	7.566 (2)		
Bond Angles (°) in Host 2b			
Cl-Sn-C(1)	99.4 (4)	Cl-Sn-C(5)	101.1 (4)
Cl-Sn-C(9)	104.6 (3)	C(1)-Sn-C(5)	115.8 (5)
C(1)-Sn-C(9)	115.5 (5)	C(5)-Sn-C(9)	116.6 (5)
Interatomic Distances (Å) in Complex 3			
Sn(1)-Cl(1)	2.745 (5)	Sn(1)-Cl(2)	2.610 (5)
Sn(2)-Cl(2)	3.388 (5)	Sn(2)-Cl(3)	2.415 (5)
Sn(1)-C(1)	2.11 (2)	Sn(1)-C(9)	2.10 (2)
Sn(1)-C(17)	2.14 (2)	Sn(2)-C(8)	2.10 (2)
Sn(2)-C(16)	2.11 (2)	Sn(2)-C(24)	2.15 (3)
Sn(1)-Sn(2)	5.993 (3)		
Bond Angles (°) in Complex 3			
Cl(1)-Sn(1)-Cl(2)	176.4 (2)	Cl(1)-Sn(1)-C(1)	88.2 (5)
Cl(1)-Sn(1)-C(9)	88.3 (6)	Cl(1)-Sn(1)-C(17)	92.2 (6)
Cl(2)-Sn(1)-C(1)	95.3 (5)	Cl(2)-Sn(1)-C(9)	88.9 (6)
Cl(2)-Sn(1)-C(17)	92.2 (6)	Cl(2)-Sn(2)-Cl(3)	177.5 (2)
Cl(2)-Sn(2)-C(8)	79.7 (7)	Cl(2)-Sn(2)-C(16)	78.8 (6)
Cl(2)-Sn(2)-C(24)	79.8 (6)	Cl(3)-Sn(2)-C(8)	102.7 (7)
Cl(3)-Sn(2)-C(16)	99.3 (6)	Cl(3)-Sn(2)-C(24)	99.8 (7)
C(1)-Sn(1)-C(9)	127.4 (9)	C(1)-Sn(1)-C(17)	114 (1)
C(9)-Sn(1)-C(17)	118 (1)	C(8)-Sn(2)-C(16)	114 (1)
C(8)-Sn(2)-C(24)	116 (1)	C(16)-Sn(2)-C(24)	120 (1)

Table 2. Kinetic Values for Exchange of Chloride Within Complex 3.^a

temp, °C	$\Delta\delta = 140 \text{ ppm}$ ($10^{-6} \text{ s} \times k_{ex}$)	$\Delta\delta = 265 \text{ ppm}$ ($10^{-6} \text{ s} \times k_{ex}$)
-20	20	70
-40	9	30
-60	3	9
-80	1	4
-100	0.15	0.4

^aResults from line shape analysis using a two site exchange model.

Table 3. Selected Interatomic Distances and Bond Angles for Host 2a and Complex 4.

Interatomic Distances (Å) in Host 2a			
Sn(1)-Cl(1)	2.36 (2)	Sn(1)-C(1)	2.03 (3)
Sn(1)-C(7)	2.26 (3)	Sn(1)-C(13)	2.10 (4)
Sn(2)-Cl(2)	2.39 (2)	Sn(2)-C(6)	2.01 (4)
Sn(2)-C(12)	2.21 (3)	Sn(2)-C(18)	2.17 (5)
Sn-Sn	5.25		

Bond Angles (°) in Host 2a			
Cl(1)-Sn(1)-C(1)	103 (1)	Cl(1)-Sn(1)-C(7)	99 (8)
Cl(1)-Sn(1)-C(13)	103 (1)	Cl(2)-Sn(2)-C(6)	103 (1)
Cl(2)-Sn(2)-C(12)	106 (1)	Cl(2)-Sn(2)-C(18)	104 (2)
C(1)-Sn(1)-C(7)	106 (1)	C(1)-Sn(1)-C(13)	125 (2)
C(7)-Sn(1)-C(13)	117 (2)	C(6)-Sn(2)-C(12)	115 (1)
C(6)-Sn(2)-C(18)	110 (2)	C(12)-Sn(2)-C(18)	118 (1)

Interatomic Distances (Å) in Complex 4			
Sn(1)-Cl(1)	2.66 (1)	Sn(2)-Cl(2)	2.57 (1)
Sn(1)-F	2.12 (4)	Sn(2)-F	2.28 (4)
Sn(1)-C(1)	2.23 (6)	Sn(1)-C(7)	2.25 (6)
Sn(1)-C(13)	2.32 (6)	Sn(2)-C(6)	2.16 (6)
Sn(2)-C(12)	2.08 (4)	Sn(2)-C(18)	2.16 (4)
Sn(1)-Sn(2)	4.40		

Bond Angles (°) in Complex 4			
Cl(1)-Sn(1)-F	173 (1)	Cl(2)-Sn(2)-F	175 (1)
Cl(1)-Sn(1)-C(1)	84 (1)	Cl(1)-Sn(1)-C(7)	83 (1)
Cl(1)-Sn(1)-C(13)	100 (1)	F-Sn(1)-C(1)	92 (2)
F-Sn(1)-C(7)	95 (2)	F-Sn(1)-C(13)	87 (1)
Cl(2)-Sn(2)-C(6)	97 (1)	Cl(2)-Sn(2)-C(12)	96 (1)
Cl(2)-Sn(2)-C(18)	82 (1)	F-Sn(2)-C(6)	83 (2)
F-Sn(2)-C(12)	89 (2)	F-Sn(2)-C(18)	93 (1)
C(1)-Sn(1)-C(7)	120 (2)	C(1)-Sn(1)-C(13)	116 (2)
C(7)-Sn(1)-C(13)	123 (2)	C(6)-Sn(2)-C(12)	116 (2)
C(6)-Sn(2)-C(18)	115 (2)	C(12)-Sn(2)-C(18)	128 (2)

Table 4. Kinetic Values for Exchange of Fluoride Within Complex 4.^a

temp. °C	$\Delta\delta = 45,000 \text{ Hz}$	$\Delta\delta = 300 \text{ Hz}$
	$(10^{-7} \text{ s} \times k_{ex})$	$(10^{-5} \text{ s} \times k_{ex})$
0	5.0	3.5
-10	4.5	3.0
-20	3.5	2.5
-30	3.0	2.0
-40	2.5	1.5
-50	1.5	1.0

^aResults from line shape analysis using a two site exchange model.

Table 5. Summary of X-ray Diffraction Data.

Compound	2b	3	2a	4
formula	$C_{24}H_{48}Cl_2Sn_2$	$C_{49}H_{70}Cl_3PSn_2$	$C_{18}H_{36}Cl_2Sn_2$	$C_{34}H_{72}Cl_2FNSn_2$
molecular weight	644.93	1033.80	560.77	822.23
crystal system	Monoclinic	Monoclinic	Monoclinic	Monoclinic
space group	C2/c (#15)	P2 ₁ /n (#14)	Pn (#7)	Pa (#7)
a, Å	18.292(5)	19.135(7)	10.742(7)	15.46(1)
b, Å	13.181(4)	9.825(2)	8.992(3)	9.118(5)
c, Å	12.763(3)	27.189(8)	11.562(2)	16.15(1)
β , deg	108.10(2)	104.10(3)	96.79(3)	116.99(5)
V, Å ³	2925(3)	4958(3)	1109(1)	2029(3)
Z	4	4	2	2
Density(calc), g/cm ³	1.46	1.38	1.68	1.35
Temp, K	296	296	296	296
F(000)	1304	2120	556	852
diffractometer	Nicolet R3m/V	Rigaku AFC5R	Rigaku AFC5R	Rigaku AFC5R
radiation ^a	Mo K α	Mo K α	Mo K α	Mo K α
μ (Mo K α), cm ⁻¹	19.07	12.36	24.97	13.93
scan type	2 θ - ω	ω ^b	2 θ - ω	ω ^b
scan speed, deg/min	2.03 to 29.30	4.0	16.0 in ω ^c	4.0
2 θ range, deg	4.0 to 50	1.5 to 50	3.5 to 50.1	2.5 to 45.0
no. of unique data	2597	9602	1968	2441
reflections ^d	1363(I > 3 σ (I))	2182(I > 3 σ (I))	1968 ^e	681(I > 3 σ (I))
no. of variables	127	371	197	189
R, R _w	0.056, 0.052	0.055, 0.054	0.069, 0.107	0.060, 0.059
largest peak ^f , eÅ ⁻³	1.01	0.47	1.57	0.48
goodness of fit	3.22	1.4	0.92	1.5

^aGraphite monochromated. ^bLehmann-Larsen profile analysis. ^cUp to three scans for weak data.

^dNumber of reflections used in refinement. ^eAll data used. ^fLargest peak in the final difference map.

Table 6. Positional Parameters and Equivalent Isotropic Thermal Parameters for $\text{Sn}_2\text{Cl}_2(\text{C}_8\text{H}_{16})_3$ (**2b**).

atom	x	y	z	$B_{\text{eq}}, \text{\AA}^2$
Sn	0.34825(4)	0.28749(8)	0.39482(6)	8.11(4)
Cl	0.2313(2)	0.3694(3)	0.3876(3)	11.2(2)
C(1)	0.3831(7)	0.381(1)	0.284(1)	10.9(8)
C(2)	0.343(1)	0.366(2)	0.167(1)	19(1)
C(3)	0.362(1)	0.393(2)	0.085(2)	20(2)
C(4)	0.348(1)	0.364(2)	-0.022(2)	17(2)
C(5)	0.3090(7)	0.144(1)	0.337(1)	10.9(8)
C(6)	0.3667(8)	0.063(1)	0.354(1)	10.9(8)
C(7)	0.4203(8)	0.072(1)	0.280(1)	9.6(7)
C(8)	0.4772(9)	-0.010(1)	0.290(1)	12(1)
C(9)	0.4162(6)	0.298(1)	0.561(1)	9.2(7)
C(10)	0.500(1)	0.327(1)	0.581(1)	11.1(9)
C(11)	0.5440(9)	0.264(1)	0.533(1)	13(1)
C(12)	0.629(1)	0.281(2)	0.559(2)	17(2)

Table 7. Positional Parameters and Equivalent Isotropic Thermal Parameters for $\text{Sn}_2\text{Cl}_2(\text{C}_6\text{H}_{12})_3$ (**2a**).

atom	x	y	z	$B_{\text{eq}}, \text{\AA}^2$
Sn(1)	0.7579	0.3373(3)	0.1899	4.1(1)
Sn(2)	1.2793(1)	0.3387(3)	0.2462(1)	4.1(2)
Cl(1)	0.570(1)	0.354(2)	0.062(2)	7.6(6)
Cl(2)	1.472(1)	0.355(2)	0.371(2)	7.2(6)
C(1)	0.741(4)	0.141(4)	0.272(3)	5(1)
C(2)	0.866(3)	0.088(3)	0.347(3)	4(1)
C(3)	0.908(3)	0.177(4)	0.445(3)	3(1)
C(4)	1.046(4)	0.142(4)	0.510(3)	3(1)
C(5)	1.144(4)	0.149(3)	0.437(3)	4(1)
C(6)	1.151(4)	0.314(4)	0.361(4)	4(1)
C(7)	0.895(3)	0.297(5)	0.062(3)	4(1)
C(8)	0.885(3)	0.159(4)	0.020(3)	4(1)
C(9)	0.983(5)	0.126(5)	-0.077(4)	7(2)
C(10)	1.108(3)	0.179(4)	-0.031(3)	4(1)
C(11)	1.173(3)	0.082(4)	0.077(3)	5(2)
C(12)	1.299(3)	0.144(4)	0.132(3)	3(1)
C(13)	0.769(6)	0.546(5)	0.274(4)	8(2)
C(14)	0.833(3)	0.671(4)	0.212(2)	6(1)
C(15)	0.967(2)	0.733(2)	0.223(2)	7(1)
C(16)	1.062(2)	0.624(2)	0.196(2)	4(1)
C(17)	1.193(4)	0.671(3)	0.228(4)	9(2)
C(18)	1.262(5)	0.556(6)	0.167(4)	6(2)

Table 8. Positional Parameters and Equivalent Isotropic Thermal Parameters for the Tin Species in $[\text{Sn}_2\text{Cl}_2(\text{C}_8\text{H}_{16})_3\cdot\text{Cl}][(\text{C}_6\text{H}_5)_3(\text{C}_6\text{H}_5\text{CH}_2)\text{P}]$ (3).

atom	x	y	z	$B_{\text{eq}}, \text{\AA}^2$
Sn(1)	0.50896(8)	0.1618(1)	0.30154(5)	4.96(7)
Sn(2)	0.55435(8)	0.2392(2)	0.09291(5)	5.94(8)
Cl(1)	0.4901(3)	0.1541(6)	0.3984(2)	6.5(3)
Cl(2)	0.5251(3)	0.1855(6)	0.2093(2)	7.3(3)
Cl(3)	0.5700(3)	0.2821(6)	0.0088(2)	8.8(4)
C(1)	0.557(1)	-0.033(2)	0.3145(7)	6(1)
C(2)	0.637(2)	-0.038(2)	0.3420(8)	8(2)
C(3)	0.688(1)	0.034(2)	0.317(1)	8(1)
C(4)	0.690(1)	-0.023(2)	0.265(1)	8(1)
C(5)	0.735(1)	0.059(3)	0.238(1)	10(2)
C(6)	0.736(2)	0.019(3)	0.186(1)	13(2)
C(7)	0.677(2)	0.056(3)	0.147(1)	12(2)
C(8)	0.661(1)	0.211(3)	0.1356(9)	10(2)
C(9)	0.560(1)	0.351(2)	0.3189(8)	8(1)
C(10)	0.510(3)	0.468(3)	0.303(2)	21(3)
C(11)	0.511(2)	0.574(4)	0.282(1)	15(3)
C(12)	0.556(1)	0.605(3)	0.246(1)	10(2)
C(13)	0.512(1)	0.651(2)	0.196(1)	11(2)
C(14)	0.541(1)	0.655(3)	0.153(1)	11(2)
C(15)	0.569(1)	0.523(3)	0.1368(8)	9(2)
C(16)	0.508(1)	0.427(2)	0.1061(8)	8(1)
C(17)	0.394(1)	0.158(3)	0.2756(7)	8(1)
C(18)	0.364(2)	0.020(4)	0.261(1)	12(2)
C(19)	0.368(2)	-0.042(3)	0.216(2)	14(3)
C(20)	0.336(2)	0.019(3)	0.164(1)	13(2)
C(21)	0.359(2)	-0.051(4)	0.125(1)	20(3)
C(22)	0.362(2)	0.002(4)	0.078(2)	16(3)
C(23)	0.408(2)	0.110(4)	0.078(1)	14(2)
C(24)	0.489(2)	0.059(3)	0.078(1)	11(2)

Table 9. Positional Parameters and Equivalent Isotropic Thermal Parameters for the Tin Species in $[\text{Sn}_2\text{Cl}_2(\text{C}_6\text{H}_{12})_3\cdot\text{F}][(\text{C}_4\text{H}_9)_4\text{N}]$ (**4**).^a

atom	x	y	z	$B_{\text{eq}}, \text{\AA}^2$
Sn(1)	0.4419	0.1118(6)	0.3566	5.8(2)
Sn(2)	0.2721(3)	0.1100(6)	0.0522(3)	4.8(2)
Cl(1)	0.538(1)	0.127(3)	0.541(1)	9(1)
Cl(2)	0.165(1)	0.090(2)	-0.124(1)	6.5(8)
F	0.355(3)	0.119(2)	0.210(3)	3.5(8)
C(1)	0.311(4)	0.103(8)	0.382(2)	6(2)
C(2)	0.267(4)	0.275(6)	0.367(3)	5(2)
C(3)	0.242(4)	0.346(6)	0.262(3)	6(2)
C(4)	0.152(4)	0.232(6)	0.199(3)	6(2)
C(5)	0.142(4)	0.318(6)	0.099(3)	5(2)
C(6)	0.220(4)	0.322(6)	0.069(4)	7(2)
C(7)	0.516(4)	0.327(6)	0.365(4)	6(2)
C(8)	0.609(4)	0.304(6)	0.340(4)	6(2)
C(9)	0.568(3)	0.255(5)	0.245(3)	4(1)
C(10)	0.496(4)	0.318(6)	0.144(3)	5(2)
C(11)	0.462(4)	0.238(6)	0.065(3)	6(2)
C(12)	0.404(3)	0.108(6)	0.047(3)	3(1)
C(13)	0.500(3)	-0.111(7)	0.333(3)	4(1)
C(14)	0.457(3)	-0.248(5)	0.325(3)	2(1)
C(15)	0.378(4)	-0.251(6)	0.256(3)	6(2)
C(16)	0.377(3)	-0.237(6)	0.157(3)	5(2)
C(17)	0.250(4)	-0.214(6)	0.050(4)	7(2)
C(18)	0.186(3)	-0.075(5)	0.054(3)	3(1)

^aAll carbon atoms refined isotropically.

TECHNICAL REPORT DISTRIBUTION LIST, GEN

	<u>No. Copies</u>	
Office of Naval Research Attn: Code 1113 800 N. Quincy Street Arlington, Virginia 22217-5000	2	Dr. David Young Code 334 NORDA NSTL, Mississippi 39529
Dr. Bernard Douda Naval Weapons Support Center Code 50C Crane, Indiana 47522-5050	1	Naval Weapons Center Attn: Dr. Ron Atkins Chemistry Division China Lake, California 93555
Naval Civil Engineering Laboratory Attn: Dr. R. W. Drisko, Code L52 Port Hueneme, California 93401	1	Scientific Advisor Commandant of the Marine Corps Code RD-1 Washington, D.C. 20380
Defense Technical Information Center Building 5, Cameron Station Alexandria, Virginia 22314	12 high quality	U.S. Army Research Office Attn: CRD-AA-IP P.O. Box 12211 Research Triangle Park, NC 27709
DTNSRDC Attn: Dr. H. Singerman Applied Chemistry Division Annapolis, Maryland 21401	1	Mr. John Boyle Materials Branch Naval Ship Engineering Center Philadelphia, Pennsylvania 19112
Dr. William Tolles Superintendent Chemistry Division, Code 6100 Naval Research Laboratory Washington, D.C. 20375-5000	1	Naval Ocean Systems Center Attn: Dr. S. Yamamoto Marine Sciences Division San Diego, California 91232

ABSTRACTS DISTRIBUTION LIST 053

Dr. M. F. Hawthorne
Department of Chemistry
University of California
Los Angeles, California 90024

Professor O. T. Beachley
Department of Chemistry
State University of New York
Buffalo, New York 14214

Dr. W. Hatfield
Department of Chemistry
University of North Carolina
Chapel Hill, North Carolina 27514

Professor R. Wells
Department of Chemistry
Duke University
Durham, North Carolina 27706

Professor K. Neidenzu
Department of Chemistry
University of Kentucky
Lexington, Kentucky 40506

Dr. Herbert C. Brown
Department of Chemistry
Purdue University
West Lafayette, IN 47907

Dr. J. Zuckerman
Department of Chemistry
University of Oklahoma
Norman, Oklahoma 73019

Professor R. Neilson
Department of Chemistry
Texas Christian University
Fort Worth, Texas 76129

Professor M. Newcomb
Department of Chemistry
~~Texas A&M University~~
College Station, Texas 77843

Professor L. Miller
Department of Chemistry
University of Minnesota
Minneapolis, Minnesota 55455

Professor K. O. Christie
Rockwell International
Canoga Park, California 91304

Dr. Margaret C. Etter
Department of Chemistry
University of Minnesota
Minneapolis, MN 55455